Trajectory Design for UAV Assisted Wireless Networks

Yao Tang, Man Hon Cheung, and Tat-Ming Lok

Abstract—Unmanned aerial vehicles (UAVs) can enhance the performance of cellular networks, due to their high mobility and efficient deployment. In this paper, we consider a single-UAV assisted wireless communication system, where the UAV is deployed as an aerial base station (BS) to serve ground users. We maximize the transmission rate of ground users in the downlink communication by optimizing the UAV trajectory. To account for the impact of the ground BS on the UAV trajectory design, we provide a higher reward for the UAV to serve at a cell edge position. The cost function takes into account both the energy consumption during moving and hovering. We formulate our problem as a route selection problem in an acyclic directed graph, where each vertex and each edge are associated with a reward and a cost, respectively. The shortest path (SP) scheme is used to determine the optimal trajectory. Simulation results show that the SP scheme achieves the highest payoff among the compared schemes. Finally, we provide an application scenario based on our campus map to illustrate how the UAV determines the optimal trajectory under the SP scheme.

I. INTRODUCTION

A. Motivations

Unmanned aerial vehicles (UAVs) are expected to be deployed in the fifth generation (5G) wireless networks [1], [2]. One typical example is the use of UAVs as aerial base stations (BSs), which can boost the capacity and the coverage of the existing cellular networks [3]–[5]. The key reasons for potential performance enhancement are their high mobility and efficient deployment. These features enable UAVs to achieve high probabilities of establishing line-of-sight (LOS) connections towards ground users, which improves the quality of service (QoS) [6], [7]. UAVs can be deployed to provide Internet coverage to rural areas or cell edges with weak signals from the ground base stations. In addition, they can provide extra service capacity for temporary events, such as major sports events and outdoor activities [1]. Yet another application is that they can be used for restoring communications in emergency situations [8]. Actually, some technology companies have already been working on UAVs. Google has launched the Loon Project [9] with the intention to provide Internet access worldwide. Moreover, UAVs as flying cell sites have been used to provide cellular coverage as part of disaster recovery operations, such as Hurricane Maria of Puerto Rico in 2017 [8].

To support the deployment of UAVs, the 3rd Generation Partnership Project (3GPP) has studied how the current cellular networks can accommodate UAVs as well as provide services that can help address areas of concern in a convenient and technically feasible way. Report [10] studied how well the LTE radio network could provide services to low altitude UAVs and the provision of 5G new radio services from high altitude platforms. All these efforts aim to combine UAVs and cellular service technologies in a mutually beneficial manner, especially under 5G wireless networks [11].

Nevertheless, to efficiently use UAVs to assist existing cellular networks, there remain a number of technical challenges, such as UAV positioning, trajectory design, and energy efficiency.

UAV deployment has been widely investigated to improve different QoS requirements by optimizing the positions and the numbers of static UAVs. The authors in [3], [4] studied the optimal altitude of a quasi-static UAV BS, which led to maximum coverage for ground users. Moreover, the minimum number of required UAV BSs to cover a given set of ground users has been studied in [5]. Besides these static UAV deployment cases, other researcher focused on the dynamic trajectory design of mobile UAVs. The work in [12] studied the throughput maximization problem by optimizing the transmission power and the single UAV trajectory in a mobile relaying system. However, the results presented in [12] showed that the UAV should fly along a rectilinear trajectory due to the constant altitude of the UAV. The work in [3] minimized the number of stop points that the UAV needed to visit in order to ensure the coverage requirements in a device-to-device communication system. However, [3] used the disk covering model, which led to a regular polygon trajectory for the UAV. Different from these constrained trajectories, the works in [6], [13] proposed more general approaches to allow trajectory design in three dimension space. The authors in [6] maximized the throughput of ground users in the downlink by optimizing the UAV-User association and power control jointly with trajectory design. Similarly, [13] studied the trajectory design, device association, and uplink power control to enable reliable uplink communications in the Internet of Things systems. However, the studies in [6] and [13] did not consider the impact of ground BSs on UAV trajectory design.

In practice, cell-edge users having weak signals from ground BSs are more likely to connect to UAVs than users within the cells. Signals from UAVs to cell-edge users are less affected by interference from ground BSs, thus enabling an improved QoS to cell-edge users. However, it does not mean that users within the cell should be excluded from UAV

Yao Tang, Man Hon Cheung, and Tat M. Lok are with the Department of Information Engineering, the Chinese University of Hong Kong (CUHK), Shatin, N.T., Hong Kong. E-mail: {ty018, mhcheung, tmlok}@ie.cuhk.edu.hk.

services. UAVs may provide extra capacity and higher data rates when there is unexpected communication congestion, such as excessive user demand. In [14], the UAV trajectory was optimized to maximize the sum data rate of cell-edge users by avoiding the interference effectively. However, the UAV can only serve regions close to cell edges, which limits the performance of users within the cell.

In this paper, we focus on how both the ground BS and user demand together affect the UAV trajectory design under the energy constraint in moving and hovering.

B. Contributions

We maximize the transmission rate of ground users in the downlink communication by optimizing the UAV trajectory. We consider that the UAV is given a priori knowledge (or prediction) of the location-and-time dependent user demand. Based on this information, the UAV can decide when and where to provide services. We provide a higher reward for the UAV to serve at a cell edge position. Actually, the reward function reflects the impact of ground BS and user demand on trajectory design. Besides, the reward function, there is also a cost function, which takes into account both the energy consumption during moving and hovering. We utilize an acyclic directed graph to illustrate our problem, where each vertex is associated with a reward, and each edge is associated with a cost. Then, we modify the graph so that both the rewards and the costs are incorporated into the newly defined edges. As a result, the Bellman-Ford algorithm can be applied to compute the optimal trajectory that maximizes the expected payoff of the UAV.

We summarize the key results and contributions as follows:

- *A general model of UAV trajectory design:* We present a general model of UAV trajectory design with a priori knowledge of location-and-time dependent user demand.
- *Graph conversion for shortest path algorithm:* We formulate the trajectory design problem, affected by ground BS, user demand and energy limitation, as a route selection problem in an acyclic directed graph. After conversion to the graph, the shortest path (SP) scheme has been provided to determine the optimal trajectory.
- *Payoff improvement:* The proposed SP scheme achieves the best performance in terms of payoff when comparing with various benchmark algorithms, namely the greedy path (GP) scheme and the circular path (CP) scheme.

II. SYSTEM MODEL

A. Regions, Time Slots, and User Demand

As shown in Fig. 1, we consider a UAV assisted wireless communication system, where the UAV works as an aerial BS for providing Internet services to a group of users located in an area. The UAV serves its associated users via time division multiple access (TDMA), and it may be connected to a nearby macro cell tower with a wireless backhaul link [15].

We divide the entire area into specific regions, such as school, company, and gymnasium. Let $\mathcal{L} = \{1, \ldots, L\}$ be
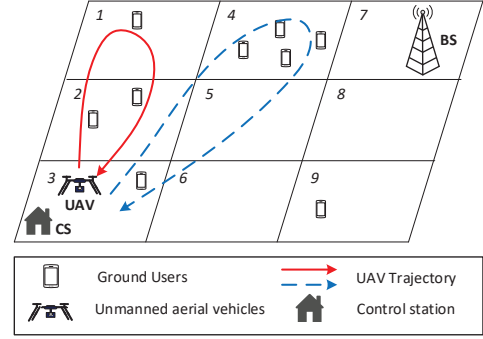

Fig. 1. An example of the UAV assisted wireless communication system. The UAV starts from control station (CS) and provides services for ground users located in $L = 9$ regions. The ground BS is located at region 7. There are two potential trajectories for the UAV. The red solid trajectory provides communication coverage for region 1 and 2, where ground users receive weak signals from the ground BS. On the other hand, the blue dashed trajectory can mitigate the communication congestion of region 4 caused by excessive user demand. In this paper, we take into account the impact of both the ground BS and the user demand for an energy-efficient trajectory design.

the set of regions, and $\mathcal{T} = \{1, \ldots, T\}$ be the set of time slots.

The UAV is given a priori knowledge of the location-and-time dependent user demand due to some events (such as concerts or sports). The UAV can access the database from the ground BS, which describes the statistics of the number of users needed to be served. Based on the demand, reward, and cost of each task (which we will define later in this section), the UAV has to decide when and where to provide wireless communication services in the T time slots. Note that the UAV starts from the control station and needs to go back at the end of the serving duration of T.

B. Tasks Model

For each region-time point, we define a task to represent it. Let $\mathcal{K} = \{1, \ldots, K\}$ be the set of tasks, where $K = LT$. We map a region-time point $(l, t), l \in \mathcal{L}, t \in \mathcal{T}$ to a task index $k \in \mathcal{K}$ by the function

$$m(l, t) = l + L(t - 1). \tag{1}$$

We describe the characteristics related to a task as follows.

Definition 1 (Task characteristics): Each task $k \in \mathcal{K}$ is associated with:

- The region $l_k \in \mathcal{L}$ and *time slot*[1] $t_k \in \mathcal{T}$.
- The reward $\rho_k \geq 0$ for completing the task (will be defined in Sec. II-D).
- The *UAV potential location*[2] $\boldsymbol{u}_k = (x_k, y_k, H_u)$, where H_u represents the constant altitude of the UAV. That is, the UAV can only be in the corresponding location while executing the task.

---

[1] Each task k is generated at the beginning of the time slot t_k. Note that the UAV must fly to the region l_k before the beginning of the time slot t_k so that it can execute the task. Otherwise, the UAV cannot work on the task.

[2] Each region is assigned a UAV potential location. When executing task k, the UAV can only stay in this location in region l_k.

- The user demand $\mathcal{I}_k = \{1, \ldots, I_k\}$, where I_k indicates the number of users in task k. We assume that the UAV knows the distribution of I_k, but not its exact value. The users are at the ground level (i.e., zero altitude), so user i's location is denoted by $\boldsymbol{v}_i = (x_i, y_i, 0), i \in \mathcal{I}_k$.

To account for the impact of the ground BS on the UAV trajectory design, we will define the reward of each task with reference to the transmission rate from the ground BS. First, we present two different channel models, on which the reward depends.

C. Channel Model

Air-to-Ground (A2G) channel model: The path between the UAV and a user can be a LOS path or a non-LOS (NLOS) path. The LOS probability, which is related to the environment, the location of the user and the UAV as well as the elevation angle, is given by [16]

$$P_{LOS}^{ki} = \frac{1}{1 + \psi \exp(-\zeta[\theta_{ki} - \psi])}, \tag{2}$$

where ψ and ζ are constant values determined by the type of environment, and θ_{ki} is the elevation angle. More specifically, $\theta_{ki} = \frac{180}{\pi} \times \sin^{-1}(\frac{H_u}{d_u^{ki}})$, where $d_u^{ki} = \|\boldsymbol{u}_k - \boldsymbol{v}_i\|$ is the Euclidean distance between the UAV and the user i. The NLOS probability is $P_{NLOS}^{ki} = 1 - P_{LOS}^{ki}$. We adopt the average channel gain model in [13]. The average channel gain between the UAV and user i is

$$g_u^{ki} = \frac{(K_0 d_u^{ki})^{-\alpha_u}}{\eta_1 P_{LOS}^{ki} + \eta_2 P_{NLOS}^{ki}}, \tag{3}$$

where $K_0 = \frac{4\pi f_c}{c}$, f_c is the carrier frequency, c is the speed of light, and α_u is the path loss exponent of the link between the UAV and the user. Besides, η_1 and η_2 ($\eta_2 > \eta_1 > 1$) are the excessive path loss coefficients in LOS and NLOS cases. As a result, the received transmission rate of user i from the UAV is

$$r_u^{ki} = \log(1 + \frac{P_u g_u^{ki}}{N_0}), \tag{4}$$

where N_0 is the power of the additive white Gaussian noise, and P_u is the transmission power of the UAV.

Ground-to-Ground (G2G) channel model: The channel between the ground BS and a user is assumed to undergo path loss and *small scale fading*[3]. The path loss is proportional to $d_b^{-\alpha_b}$, where d_b is the distance between ground BS and user i, and α_b is the path loss exponent of the link between the ground BS and the user. The power gain of small scale fading channel h_b is exponentially distributed with unit mean $h_b \sim \exp(1)$. The channel gain between the ground BS and user i is $g_b^i = h_b(d_b^i)^{-\alpha_b}$. Therefore, the received transmission rate of user i from the ground BS is

$$r_b^i = \log(1 + \frac{P_b g_b^i}{N_0}), \tag{5}$$

where P_b is the transmission power of the ground BS.

---

[3]We do not consider the small-scale fading in A2G model, because the excessive path loss is dominant [13].
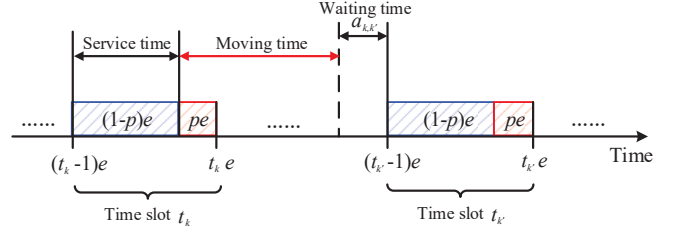

Fig. 2. Time slot structure.

D. Reward Function

To incentivize the UAV to serve at cell-edge locations and densely populated regions, we define the reward as the summation of downlink transmission rate differences $r_u^{ki} - r_b^i$ between the A2G and G2G models of all the users $i \in \mathcal{I}_k$ in the region

$$\rho_k(h_b, I_k) = \beta \Delta \sum_{i \in \mathcal{I}_k} \max\{0, r_u^{ki} - r_b^i\}, \tag{6}$$

where β denotes the coefficient of the reward, and Δ represents the fixed period of time that each user can be served by the UAV under TDMA. When $r_u^{ki} < r_b^i$, the reward will be 0, which indicates that user i will be served by the ground BS rather than the UAV. The expected reward $\mathbb{E}[\rho_k]$ can be computed by taking expectation over the number, the locations, and the channel gains of the users.

E. Cost Function

The cost function takes into account both the energy consumption during moving and hovering. Assume that the UAV aims to perform task k' after completing task k ($k', k \in \mathcal{K}$). The flying distance between these two tasks can be expressed as $d_{k,k'} = \|\boldsymbol{u}_k - \boldsymbol{u}_{k'}\|$. By considering that the UAV flies at a constant speed ϕ, the moving time is $\xi_{k,k'} = \frac{d_{k,k'}}{\phi}$. Therefore, the hovering time is

$$\delta_{k,k'} = (t_{k'} - t_k)e - \xi_{k,k'}, \tag{7}$$

where $\delta_{k,k'} \geq 0$. We define the cost to be the sum of the moving cost and the hovering cost as

$$c_{k,k'} = \gamma_1 \xi_{k,k'} + \gamma_2 \delta_{k,k'}, \tag{8}$$

where $\gamma_1, \gamma_2 \geq 0$ represent the costs of moving and hovering per unit time. In practice, the energy consumption in moving is higher than hovering within the same duration, so $\gamma_1 \geq \gamma_2$. Thus, the cost of moving per unit time is no less than the cost of the hovering.

F. Time Slot Structure

We illustrate the time slot structure in Fig. 2 to explain how the UAV performs tasks. We let e be the length of the time slot, where a certain fraction p is reserved for the UAV movement. To obtain the reward ρ_k for each task $k \in \mathcal{K}$, the UAV needs to arrive at region l_k by time $(t_k - 1)e$ (i.e., the beginning time of slot t_k) and serve the users in the region until time $(t_k - p)e$. Thus, if the UAV is currently working on task k, it can execute task k' only if it can arrive region $l_{k'}$
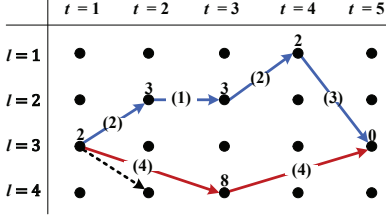
Fig. 3. An example graph $\mathcal{G}$ of UAV trajectory design. Each vertex represents one task and is associated with a reward. Each edge is associated with a cost. The edge $((3,1),(4,2))$ is not feasible. Besides, we have two feasible routes $\boldsymbol{s}_1 = ((3,1),(2,2),(2,3),(1,4),(3,5))$ and $\boldsymbol{s}_2 = ((3,1),(4,3),(3,5))$.

by time $(t_{k'} - 1)e$ after taking a moving time of $\xi_{k,k'}$. That is, we need the waiting time

$$a_{k,k'} = (t_{k'} - 1)e - (t_k - p)e - \xi_{k,k'} \geq 0. \quad (9)$$

III. Trajectory Design

In this section, we formulate the UAV trajectory design as a route selection problem in an acyclic directed graph. In Section III-A, we describe the graph representation of trajectory design. In Section III-B, we convert the graph so that we can apply the shortest path (SP) algorithm to compute the optimal trajectory.

A. Graph Representation of Trajectory Design

Based on the task characteristics in Section II-B, we define the graph associated with regions and time slots as follows.

Definition 2 (Graph representation): Let $\mathcal{G} = (\mathcal{V}, \mathcal{E})$ be a graph. We define the set of vertex $\mathcal{V}$ and the set of edge $\mathcal{E}$ as follows. The vertex set contains all the region-time points

$$\mathcal{V} = \{(l,t) : l \in \mathcal{L}, t \in \mathcal{T}\}. \quad (10)$$

The reward associated with each vertex is expected reward $\mathbb{E}[\rho_{m(l,t)}]$ defined for task $k = m(l,t)$ in Section II-D. Each edge is the link between two different region-time points as

$$\mathcal{E} = \{((l,t),(l',t')) : l,l' \in \mathcal{L}, t,t' \in \mathcal{T}, t' > t, \\ a_{m(l,t),m(l',t')} \geq 0\}. \quad (11)$$

From (9), an edge $((l,t),(l',t'))$ exists only when the waiting time is nonnegative. Each existing edge is associated with the cost $c_{m(l,t),m(l',t')}$ defined in (8).

Next, we formulate the UAV trajectory design as a region-time route selection problem in graph $\mathcal{G}$. We define the UAV's feasible routes as follows.

Definition 3 (Feasible route): Based on graph $\mathcal{G}$, feasible route of the UAV is

$$\boldsymbol{s} = ((l^1,t^1),(l^2,t^2),\ldots,(l^n,t^n)) \in \mathcal{S}, \quad (12)$$

where the vertex $(l^j,t^j) \in \mathcal{V}, \forall j = 1,\ldots,n$, and the edge $((l^j,t^j),(l^{j+1},t^{j+1})) \in \mathcal{E}, \forall j = 1,\ldots,n-1$. For the first region-time point (l^1,t^1), l^1 represents the source and $t^1 = 1$. For the last region-time point (l^n,t^n), l^n represents the destination and $t^n = T$.
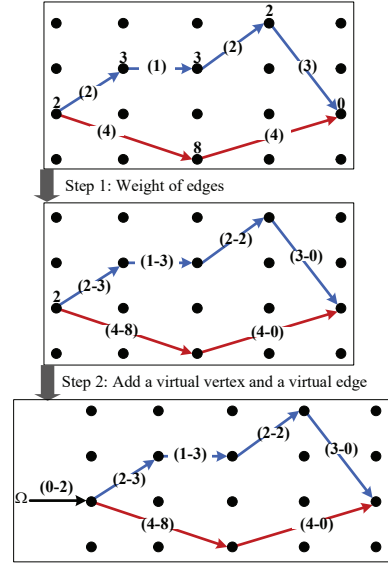

Fig. 4. An illustration of the graph conversion from graph $\mathcal{G}$ into graph $\mathcal{G}^*$.

We show an example in Fig. 3. We can see that the edge $((3,1),(4,2))$ is not feasible, because the UAV cannot arrive in region 4 before the beginning of the second time slot. Besides, we have two feasible routes $\boldsymbol{s}_1 = ((3,1),(2,2),(2,3),(1,4),(3,5))$ and $\boldsymbol{s}_2 = ((3,1),(4,3),(3,5))$. In this example, the source and destination are both in the *same*[4] region 3.

Let $\mathcal{V}(\boldsymbol{s})$ and $\mathcal{E}(\boldsymbol{s})$ denote the set of vertices and edges traversed by the route $\boldsymbol{s}$. The goal of the trajectory design is to maximize its payoff as

$$\max_{\boldsymbol{s} \in \mathcal{S}} \quad U(\boldsymbol{s}) = \sum_{(l,t) \in \mathcal{V}(\boldsymbol{s})} \mathbb{E}[\rho_{m(l,t)}] - \\ \sum_{((l,t),(l',t')) \in \mathcal{E}(\boldsymbol{s})} c_{m(l,t),m(l',t')}. \quad (13)$$

Note that the vertex of graph $\mathcal{G}$ is associated with a reward, so we cannot directly apply a standard *shortest path algorithm*[5] to solve problem (13).

B. Graph Conversion and Shortest Path (SP) Scheme

In this subsection, we convert graph $\mathcal{G}$ into a new graph $\mathcal{G}^*$, and apply the Bellman-Ford algorithm to find the *optimal* route in problem (13), which takes the following steps.

1) *The weight of edges:* The newly defined edges incorporate both the rewards and the costs, where the weight of an edge in graph $\mathcal{G}^*$ as

$$w_{m(l,t),m(l',t')} = c_{m(l,t),m(l',t')} - \mathbb{E}[\rho_{m(l',t')}]. \quad (14)$$

Then, we will not associate any reward with the vertices.

2) *Add a virtual vertex and a virtual edge to graph $\mathcal{G}^*$:* The UAV sets off from the control station. We have the

[4]Note that the proposed shortest path (SP) scheme is suitable for arbitrary source and destination.

[5]We use Bellman-Ford algorithm, because it can compute shortest path on a graph with both positive and negative edge weight.

reward of the starting point $\mathbb{E}[\rho_{m(l^1,t^1)}]$ defined in (12). We use Ω to represent the virtual vertex, and add a virtual edge to connect it with the starting point (see the third subfigure in Fig. 4). Therefore, the weight of this virtual edge is $-\mathbb{E}[\rho_{m(l^1,t^1)}]$. We use ϵ to represent this virtual edge. Fig. 4 illustrates how these two steps convert graph $\mathcal{G}$ into graph $\mathcal{G}^*$.

3) *Run Bellman-Ford Algorithm:* Based on graph $\mathcal{G}^*$, the Bellman-Ford algorithm [17] is applied to find the optimal route $\boldsymbol{s}^*$.

4) *Conversion from cost minimization to payoff maximization:* The minimal cost computed by the Bellman-Ford algorithm is opposite to the maximum payoff. That is,

$$U(\boldsymbol{s}^*) = - \sum_{((l,t),(l',t'))\in\mathcal{E}(\boldsymbol{s}^*)\cup\epsilon} w_{m(l,t),m(l',t')}. \quad (15)$$

Proposition 1: The UAV can determine its optimal route $\boldsymbol{s}$ within $\mathcal{O}(K^3)$ time.

IV. PERFORMANCE EVALUATIONS

In this section, we evaluate the performance of our proposed SP scheme by comparing it with the two benchmark schemes under various system parameters. We also present a potential application example based on our campus map.

A. Simulation Setting

For our simulations, the UAV provides services for a geographical area of size 1 km × 1 km. As shown in Fig. 1, we divide the entire area into $L = 9$ square regions with 333.3 m side length. We consider $T = 20$ time slots. Therefore, the total number of tasks is $K = LT = 180$. Moreover, we suppose UAV potential location $\boldsymbol{u}_k$ is the center of each region l_k. The ground BS is located in region 7, and the UAV control station is in region 3 (see Fig. 1). Ground users are randomly distributed in 9 regions according to a Gaussian distribution with mean μ_k and variance σ_k^2, and their location changes over duration T. Besides, the certain fraction p of each time slot reserved for the UAV movement is 0.5. Other simulation parameters are listed in Table I.

B. Benchmark Schemes

In our simulation, we compare our SP scheme with two benchmark schemes.

Greedy path (GP) scheme: In the GP scheme, we assume that the UAV only considers the user demand one-time slot ahead. More specifically, for each time slot t, the GP scheme aims to find the next optimal region that maximizes it payoff, which can be formulated as

$$\begin{aligned} \underset{l'\in\mathcal{L}}{\arg\max} \quad & \mathbb{E}[\rho_{m(l',t+1)}] - c_{m(l,t),m(l',t+1)} \\ \text{subject to} \quad & a_{m(l,t),m(l',t+1)} \geq 0. \end{aligned} \quad (16)$$

Circular path (CP) scheme: In the CP scheme, the UAV provides services for each region periodically during the duration of T [18], [19]. In the simulations, we assume that the UAV serves the regions in a periodic manner in the order of region $3, 2, 1, 4, 7, 8, 9, 5, 6, 3$.

TABLE I
SYSTEM PARAMETERS

Parameter	Description	Value
P_b	Transmission power of BS	49 dBm [10]
P_u	Transmission power of UAV	26 dBm [10]
H_b	Altitude of the BS	25 m [10]
H_u	Altitude of the UAV	90 m [10]
f_c	Carrier frequency	2 GHz [10]
N_0	Noise power	-96 dBm [10]
α_u	Path-loss exponent UAV-User	2 [20]
α_b	Path-loss exponent BS-User	4 [20]
η_1, η_2	Path-loss for LOS, NLOS	$3, 23$ dB [10], [20]
ψ, ζ	Environment parameters	$11.95, 0.14$ [20]

C. Performance Analysis

Impact of movement speed: In Fig. 5, we plot the UAV payoff against the movement speed ϕ. We can see that the SP scheme achieves the highest payoff among all three schemes. Also, the payoff increases with the movement speed under the SP scheme and the GP scheme. This is because the UAV has more feasible routes as speed ϕ increases, and more tasks can be served by the UAV. However, due to the circular trajectory, the UAV may miss many tasks with high rewards under the CP scheme, which leads to the lowest payoff.

Impact of movement coefficient: Fig. 6 shows that the payoff decreases with the movement coefficient γ_1. Higher movement coefficient increases the movement cost, and the UAV prefers staying in one region than serving different regions. Due to more feasible routes, the SP scheme has a higher payoff than other schemes under the same movement coefficient.

Impact of user demand variance: To characterize the impact of uncertainty of the user demand I_k, we define the payoff ratio as the expected payoff (with only the incomplete information of the distribution of I_k) divided by the actual payoff (with the complete information of the exact value of I_k). The mean of the user demand is $\mu_k = 50$ for all $k \in \mathcal{K}$, and the variance is $\sigma_k^2 \in [0, 50]$. From Fig. 7, we can observe that the SP scheme has a higher payoff ratio than other schemes under the same variance. It indicates that the SP scheme is more resilient on the uncertainty of user demand.

D. Potential Application Example

We introduce a concrete example based on the campus map. We consider $L = 9$ regions and $T = 5$ time slots. Therefore, the total task number should be $K = LT = 45$. For the simplicity of illustration, we only consider 5 tasks on the map. The information about each task has been shown in Fig. 8, such as generation time, region, and user demand. As we can see, the UAV serving order under the SP scheme is $(z, 1, 3, 4, 5, z)$, where z represents the UAV control station. Task 2 has not been executed in 5 time slots, because Task 2 is far away from Task 1 and Task 3. It is the better choice for the UAV to wait for Task 3. Based on the actual distance between these tasks, we calculate the UAV payoff. The performance of the three schemes is summarized in Table II. We can see that the SP scheme achieves the highest payoff.
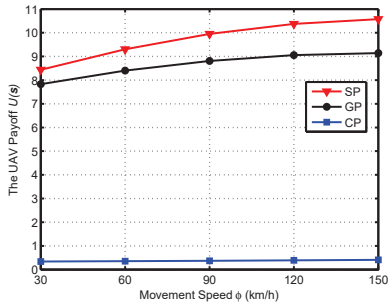
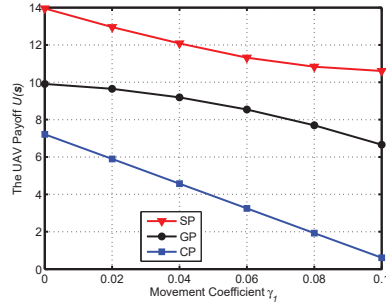Fig. 5. Payoff for movement speed with $\beta = 0.07$, $\gamma_1 = 0.07$, and $\gamma_2 = 0.05$.

Fig. 6. The impact of movement coefficient on total payoff with $\beta = 0.07$ and $\gamma_2 = 0.05$.
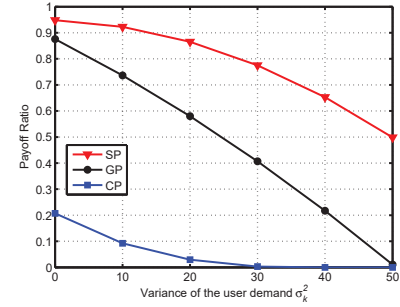

Fig. 7. The impact of user demand variance with $\mu_k = 50$ and $\phi = 30$ km/h.

Fig. 8. A potential application example of the UAV trajectory based on our campus map under the SP scheme.

TABLE II
PERFORMANCE COMPARISON IN THE POTENTIAL EXAMPLE

Schemes	SP	GP	CP
Payoff	53.1	46.1	16.5
Trajectory	$(z, 1, 3, 4, 5, z)$	$(z, 3, 4, 5, z)$	$(z, 5, 2, 3, 4, 1, z)$

V. CONCLUSION

In this paper, we considered the impact of both the ground BS and user demand on the energy-efficient UAV trajectory design. Specifically, we provided a higher reward for the UAV to serve in a region at the cell edge or with a high user demand. We used a cost function to capture both the energy consumption during moving and hovering. We formulated UAV trajectory design as a route selection problem in an acyclic directed graph. We proposed a graph conversion for the shortest path (SP) scheme to determine the optimal trajectory that maximizes the UAV's payoff. Simulation results showed that our SP scheme achieves the highest payoff comparing with other benchmark schemes.

In the future work, we will consider the impact of cooperative multi-UAVs in more general and practical system scenarios, such as multi-UAVs with their positions automatically updated with the real-time user demand.

REFERENCES

[1] M. Mozaffari, W. Saad, M. Bennis, Y. Nam, and M. Debbah, "A tutorial on UAVs for wireless networks: Applications, challenges, and open problems," *IEEE Communications Surveys & Tutorials (to appear)*, 2019.

[2] G. Geraci, A. Garcia-Rodriguez, L. G. Giordano, D. López-Pérez, and E. Björnson, "Understanding UAV cellular communications: From existing networks to massive MIMO," *IEEE Access*, vol. 6, pp. 67 853–67 865, Nov. 2018.

[3] M. Mozaffari, W. Saad, M. Bennis, and M. Debbah, "Unmanned aerial vehicle with underlaid device-to-device communications: Performance and tradeoffs," *IEEE Trans. Wirel. Commun*, vol. 15, no. 6, pp. 3949–3963, Jun. 2016.

[4] A. Al-Hourani, S. Kandeepan, and S. Lardner, "Optimal LAP altitude for maximum coverage," *IEEE Wireless Commun. Lett*, vol. 3, no. 6, pp. 569–572, Dec. 2014.

[5] J. Lyu, Y. Zeng, R. Zhang, and T. J. Lim, "Placement optimization of UAV-mounted mobile base stations," *IEEE Commun. Lett*, vol. 21, no. 3, pp. 604–607, Mar. 2017.

[6] Q. Wu, Y. Zeng, and R. Zhang, "Joint trajectory and communication design for multi-UAV enabled wireless networks," *IEEE Trans. Wireless Commun.*, vol. 17, no. 3, pp. 2109–2121, Mar. 2018.

[7] L. Gupta, R. Jain, and G. Vaszkun, "Survey of important issues in UAV communication networks," *IEEE Communications Surveys & Tutorials*, vol. 18, no. 2, pp. 1123–1152, Second quarter 2016.

[8] "Use of UAVs for restoring communications in emergency situations," White Paper, ATIS, Dec. 2018.

[9] *Project Loon.* [Online]. Available: https://www.google.com/loon

[10] 3GPP Technical Report 36.777, "Technical specification group radio access network; Study on enhanced LTE support for aerial vehicles (release 15)," Dec. 2017.

[11] "Unmanned aerial vehicle (UAV) utilization of cellular services," White Paper, ATIS, Aug. 2017.

[12] Y. Zeng, R. Zhang, and T. J. Lim, "Throughput maximization for UAV-enabled mobile relaying systems," *IEEE Trans. Commun.*, vol. 64, no. 12, pp. 4983–4996, Dec. 2016.

[13] M. Mozaffari, W. Saad, M. Bennis, and M. Debbah, "Mobile unmanned aerial vehicles (UAVs) for energy-efficient Internet of Things communications," *IEEE Trans. Wireless Commun.*, vol. 16, no. 11, pp. 7574–7589, Nov. 2017.

[14] F. Cheng, S. Zhang, Z. Li, Y. Chen, N. Zhao, F. R. Yu, and V. C. M. Leung, "UAV trajectory optimization for data offloading at the edge of multiple cells," *IEEE Trans. Veh. Technol*, vol. 67, no. 7, pp. 6732–6736, Jul. 2018.

[15] A. Fotouhi, M. Ding, and M. Hassan, "Dronecells: Improving 5G spectral efficiency using drone-mounted flying base stations," *CoRR*, vol. abs/1707.02041, 2017. [Online]. Available: http://arxiv.org/abs/1707.02041

[16] A. Al-Hourani, S. Kandeepan, and A. Jamalipour, "Modeling air-to-ground path loss for low altitude platforms in urban environments," in *Proc. IEEE GLOBECOM*, Austin, TX, USA, Dec. 2014.

[17] T. Cormen, C. Leiserson, R. Rivest, and C. Stein, *Introduction to Algorithms*. MIT Press.

[18] J. Lyu, Y. Zeng, and R. Zhang, "Spectrum sharing and cyclical multiple access in UAV-aided cellular offloading," in *Proc. IEEE GLOBECOM*, Singapore, Dec. 2017.

[19] Y. Zeng and R. Zhang, "Energy-efficient UAV communication with trajectory optimization," *IEEE Trans. Wireless Commun.*, vol. 16, no. 6, pp. 3747–3760, June 2017.

[20] 3GPP Technical Report 38.901, "Study on channel model for frequencies from 0.5 to 100 GHz (release 14)," May. 2017.